Trends and Spatio-Temporal Variability of Summer Mean and Extreme Precipitation Events across South Korea for 1973–2022

Hye-Ryeom Kim[1,3], Mincheol Moon[2,4], Junghee Yun[3,4], and Kyung-Ja Ha[1,2,3,4*]

[1]BK21 School of Earth and Environmental Systems, Pusan National University, Busan, Republic of Korea.

[2]Department of Climate System, Pusan National University, Busan, Republic of Korea.

[3]Department of Atmospheric Sciences, Pusan National University, Busan, Republic of Korea.

[4]Center for Climate Physics, Institute for Basic Science, Busan, Republic of Korea.

Corresponding author: Kyung-Ja Ha (kjha@pusan.ac.kr)

Key Points:

- Observational data are invaluable in studying extreme precipitation events.
- Extreme precipitation increased in 1973–2022, with the hourly-maximum precipitation showing a statistically significant increase.
- Extreme precipitation has a major effect on the summer rainfall in South Korea.

Abstract

Climate change has altered the frequency, intensity, and timing of mean and extreme precipitation events. Extreme precipitation has caused tremendous socio-economic losses and displays strong regional variability. Although many previous studies have addressed daily extreme precipitation, hourly extreme rainfall still needs to be thoroughly investigated. In this study, we investigated the trends, spatio-temporal variability, and long-term variations in mean and extreme precipitation over South Korea using daily and hourly observational data. During the past 50 years (1973–2022), there has been a notable escalation in maximum hourly precipitation, although the boreal summer mean precipitation has increased only marginally. Regionally, an increase in mean and extreme rainfall occurred in the northern part of the central region. Moreover, increased intensity and frequency of extreme precipitation have contributed more to the total summer precipitation in recent years. Our findings provide scientific insights into the progression of extreme summer precipitation events in South Korea.

Plain Language Summary

Climate change affects both mean and extreme precipitation events. This leads to changes in the frequency, intensity, and timing of extreme rainfall events. Extreme precipitation is inextricably linked to our human livelihoods and has the potential to cause substantial socioeconomic losses. In addition, there are large regional differences between these events. Although many previous studies have examined daily extreme precipitation, hourly extreme rainfall remained unclear. Here we investigated the trends, spatio-temporal variability, and long-term variations in mean and extreme precipitation across South Korea using daily and hourly observational data. It was important to note that hourly maximum precipitation was significantly intensified, whereas the boreal summer mean precipitation displayed a slight increase over the past 50 years (1973–2022). In terms of spatial distribution, the northern part of the central region experienced an increase in mean and extreme rainfall. Also, increased intensity and frequency of extreme precipitation have played key roles in the summertime total precipitation in recent years. Our findings provide a scientific background for understanding changes in summer extreme rainfall events in South Korea.

1 Introduction

Climate change has a significant impact on the Earth system. Globally, total human-induced surface air temperature increased by approximately 1.07 °C (0.8 °C to 1.3 °C) from 1850 to 2019 (IPCC, 2022). In tandem with rising temperatures, worldwide mean precipitation tends to increase (Allen & Ingram, 2002; Held & Soden, 2006). The frequency of heavy rainfall has increased considerably since 1951, and it varies strongly between regions and subregions (IPCC, 2022). Light precipitation events decreased in frequency, whereas heavy precipitation events increased in frequency and intensity (Trenberth et al., 2003; Alexander et al., 2006; Kharin et al., 2007; Allan & Soden, 2008; O'Gorman & Schneider, 2009; Min et al., 2011; Chou et al., 2012; Ha et al., 2020). The Intergovernmental Panel on Climate Change (IPCC) also pointed out that climate change could affect the frequency, intensity, and timing of extreme events such as heatwaves, droughts, tropical cyclones, and extreme rainfall events (IPCC, 2022). As one of the most hazardous extreme phenomena, extreme rainfall events bring considerable damage, resulting in secondary disasters including landslides and flash floods (Dave et al., 2021; Kim et al., 2021; Meyer et al., 2021; Ning et al., 2021). Extreme rainfall has a severe impact on human life, ecosystems, and the social economy of agriculture, causing colossal socioeconomic losses. Therefore, it is essential to understand extreme rainfall events.

Compared to the global mean surface warming, South Korea has experienced considerably greater surface warming because of the complex influence of several climate variabilities along the northeastern coast of Asia (Jung et al., 2002; An et al., 2011). In terms of linear trends, the local temperatures have risen by 1.90 °C (1912–2014), 1.35 °C (1954–2014), and 0.99 °C (1973–2014), which are 1.4–2.6 times greater than the global land mean temperature increases (Park et al., 2017). Regarding global warming, particularly for the Korean Peninsula (KP), a growing number of previous studies proposed that the frequency and intensity of extreme weather events (i.e., extreme precipitation events, droughts, heat waves, and tropical cyclones) have increased over the past few decades (Kim et al., 2012; Lee et al., 2012; Min et al., 2015; Ha et al., 2020; Park et al., 2021; Seo et al., 2021). This summer, the metropolitan area endured particularly heavy torrential rain and flooding. In Seoul, an hourly downpour of 141.5 mm/hr was recorded, which was the heaviest hourly precipitation breaking the record in 80 years (Bae & Yeung, 2022). In addition, this event surpassed 381.5 mm, which was the heaviest daily precipitation recorded in the past 102 years. At least 14 people died as a result of heavy rainfall, and the total sum of the damage was estimated to exceed USD 50M. Several studies have investigated the changes in mean and extreme rainfall in South Korea (Ho et al., 2003; Jung et al., 2011; Baek et al., 2017; Azam et al., 2018). Most of these studies focused on daily extreme precipitation, therefore, our understanding of hourly extreme rainfall events is insufficient. However, hourly extreme precipitation should be highlighted because it can induce great damage, as we have already experienced.

As one of the primary factors of heavy rainfall events, the Changma and typhoons greatly impact extreme precipitation, whereas the East Asian summer monsoon has a major effect on the rainy season (Lee et al., 2017). The Changma is most active between early July and early September, with the first Changma starting in late June and ending in late July (Seo et al., 2011; Park et al., 2015). In addition, the second Changma is mainly associated with typhoons in late summer, and typhoons intensively affect the KP in July, August, and September (Lee et al., 2017; Moon & Ha, 2021). Heavy rainfall in the KP during the boreal summer needs to be investigated because the sub-seasonal variability is very large, even during summer.

On the other hand, it is necessary to understand long-term variations and trends in mean and extreme precipitation in water resource and flood risk management (Moberg et al., 2006; Ha et al., 2009; Pei et al., 2017; Kim & Ha, 2021; Wang et al., 2021; Hu et al., 2022; Ryan et al., 2022). Ensemble empirical mode decomposition (EEMD) method is employed to appropriately reflect nonlinear responses to global warming and urbanization (Yun et al., 2018; Jeong et al., 2022). Hu et al., (2022) revealed that the extreme precipitation on the Tibetan Plateau and its surrounding areas is strongly correlated with the strength of the Indian Ocean and Western Pacific warm pools through the multi-time-scale analysis.

Consequently, the purpose of this study was as follows: (1) to analyze the trends of extreme precipitation in terms of hourly and daily time scales, as well as their spatial patterns over South Korea; (2) to focus on long-term variations in the mean temperature and extreme precipitation, as well as their relationships with EEMD methods; and (3) to identify the recent changes in major spatio-temporal distributions of summertime precipitation.

2 Data and Methods

2.1 Data

We used daily mean precipitation, 1-hour maximum precipitation, and daily mean temperature from the Automated Surface Observing System (ASOS) for the investigation of trends and variability in Korean summer rainfall from 1973 to 2022. Sixty stations out of a total of 103 stations were selected, encompassing the entire analysis period (Figure 1a). The months of June–July–August (JJA) are regarded as the boreal summer. Hourly precipitation data were obtained from the European Center for Medium-Range Weather Forecasts reanalysis version 5 (ERA5; Hersbach et al., 2020). We adjusted the time in line with Korea Standard Time (KST) owing to the time difference between the Universal Time Coordinate (UTC) and KST. For the ERA5 reanalysis data, the area-averaged precipitation and nearest grid point precipitation were compared to the ASOS total station mean precipitation. Instead of area-averaged precipitation, the nearest grid point precipitation corresponded more closely with the ASOS. However, since the late 1990s, the ERA5 dataset has tended to underestimate the JJA mean precipitation from the ASOS (Figure 1b). In particular, when the JJA mean precipitation was at its peak, ERA5 data could not match the observation. A heavy rainfall event is typically a localized event occurring in a small area. Therefore, ERA5, which had a spatial resolution of approximately 30km, was not sufficient to simulate these peak events in observation. This was consistent with that of Borodina et al., (2017) and highlighted the importance of observational data in studying localized heavy rainfall events. In terms of the topography, the ETOPO1 dataset was selected (Amante & Eakins, 2009).

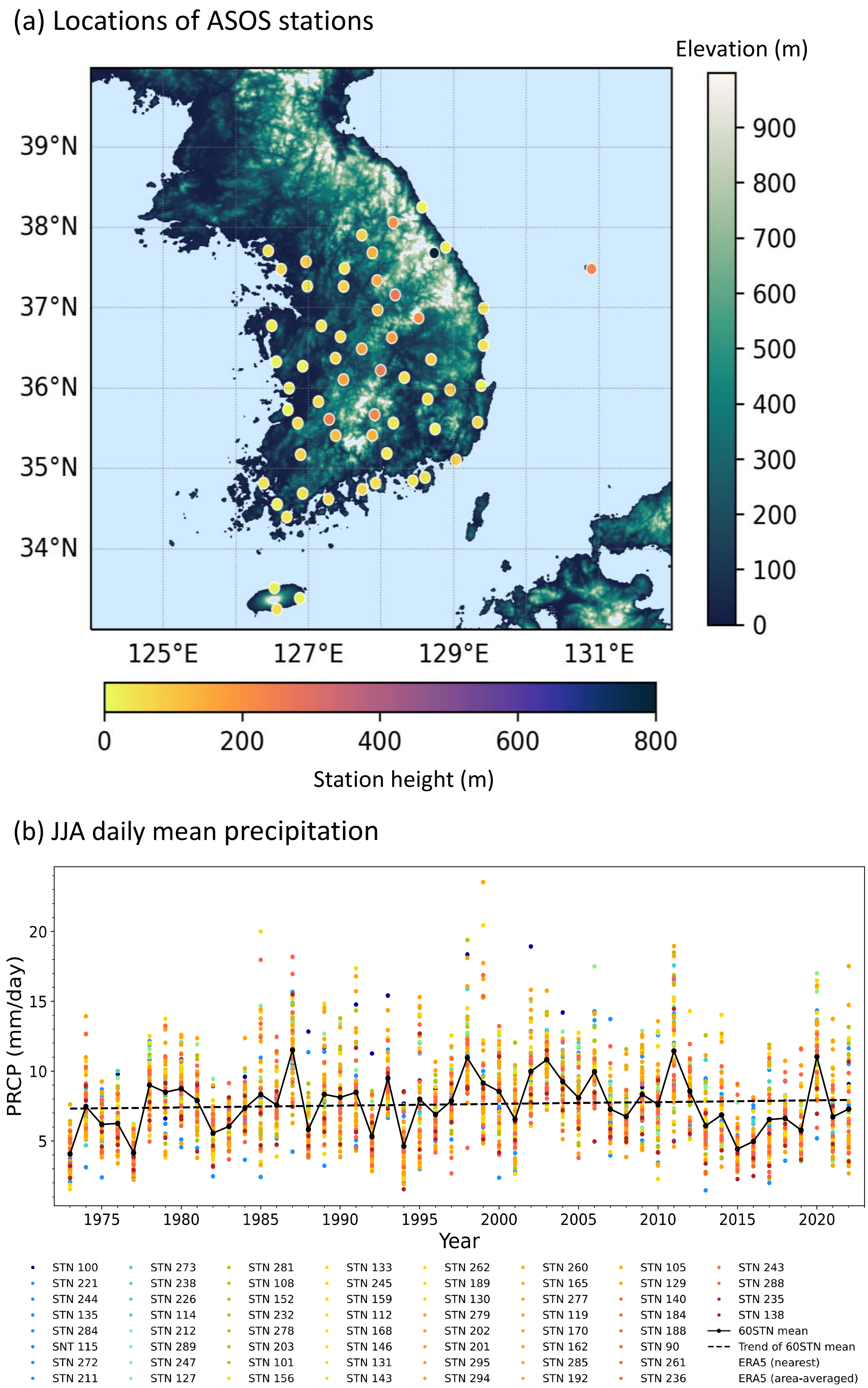

(a) Locations of ASOS stations
Elevation (m)
39°N
38°N
37°N
36°N
35°N
34°N
125°E
127°E
129°E
131°E
0 100 200 300 400 500 600 700 800 900
0 200 400 600 800
Station height (m)
(b) JJA daily mean precipitation
PRCP (mm/day)
5 10 15 20
1975 1980 1985 1990 1995 2000 2005 2010 2015 2020
Year
STN 100
STN 221
STN 244
STN 135
STN 284
SNT 115
STN 272
STN 211
STN 273
STN 238
STN 226
STN 114
STN 212
STN 289
STN 247
STN 127
STN 281
STN 108
STN 152
STN 232
STN 278
STN 203
STN 101
STN 156
STN 133
STN 245
STN 159
STN 112
STN 168
STN 146
STN 131
STN 143
STN 262
STN 189
STN 130
STN 279
STN 202
STN 201
STN 295
STN 294
STN 260
STN 165
STN 277
STN 119
STN 170
STN 162
STN 285
STN 192
STN 105
STN 129
STN 140
STN 184
STN 188
STN 90
STN 261
STN 236
STN 243
STN 288
STN 235
STN 138
60STN mean
Trend of 60STN mean
ERA5 (nearest)
ERA5 (area-averaged)

Figure 1. (a) Topographical sketch map of South Korea with 60 ASOS stations (circles, bottom colored bar). The shading displays the topographic elevation (upper-right colored bar). (b) Interannual variability in summertime (JJA) daily precipitation at each station over the past 50 years (1973–2022). The solid black line represents the JJA mean precipitation of all stations, and its trend is indicated via a black dashed line. For the ERA5 dataset, the nearest grid point of each station (solid dark olive-green line) and area-averaged value (solid yellow-green line) are also exhibited.

2.2 Extreme Indices

Five indices derived from the Expert Group on Climate Change Detection and Indices (ETCCDI) were calculated to describe the features of extreme precipitation (Table S1). A wet day indicated that the daily precipitation amount was more than 1mm (Yao et al., 2008; Kim et al., 2013). The total precipitation (PRCPTOT) was the sum of precipitation on wet days. Extremely wet day total precipitation denoted instances where the daily precipitation exceeded the 95th and 99th percentiles of the wet day precipitation (R95p, R99p); this was calculated during the summer. In addition, to compare the changes in summertime precipitation, we divided the 50 years into two periods: 1973–1992 (P1, reference period) and 2003–2022 (P2), and calculated each percentile value for the reference period. For frequency, we used the number of heavy precipitation days when the daily precipitation amount was more than 20mm (R20mm) and the number of dry days when the daily precipitation was less than 1mm. We defined the number of days with R95p and R99p as R95pF and R99pF, respectively. The hourly extreme precipitation index (RX1H) was defined as the maximum 1-hour precipitation; this index was used to focus on heavy downpours in a short period of time. In Section 3.3, we selected a high-population group with a population of more than 1,000,000 and a low-population group with a population of less than 50,000 in order to examine the effects of urbanization on extreme precipitation (Table S2).

2.3 Ensemble Empirical Mode Decomposition (EEMD)

An improved noise-assisted data analysis method, Ensemble Empirical Mode Decomposition (EEMD), decomposes the original signals ($x(t)$) into a finite number (N) of independent signals with periodicity ($C_i(t), i = 1, 2, 3, \cdots, n$) and a residual linear or nonlinear trend ($R(t)$) (Wu & Huang, 2004, 2009).

$$x(t) = \sum_{i=1}^{n} C_i(t) + R(t) \tag{1}$$

Here, the standard deviation of the added noise series and the ensemble number for EEMD were entered as 0.2 and 200, respectively.

2.4 Extended Empirical Orthogonal Function (EEOF)

The Extended Empirical Orthogonal Function Analysis (EEOF) was employed in conjunction with reanalysis data to analyze the temporal evolution of the principal spatial structure. Several previous studies have applied EEOF to investigate the evolution of the substructure (Chen & Harr, 1993; Kim et al., 2008). Using the EEOF analysis, we interpreted the substructure as the propagation or evolution of the sub-seasonal mode over time of the first substructure of the function. The eigenvector and eigenfunction for an atmospheric variable, $\mu_{ij'}^{(n)}$, were as follows:

$$\alpha_{il}^{(n)} = \sum_{j'=1}^{J'} \mu_{ij'}^{(n)} \Psi_{j'l} \quad (2)$$

where i indicates the space, j denotes the time, j' indicates the time in the window, and n represents the number of windows. $\Psi_{j'l}$ is a function of temporal variation, and α_{il} is a window-averaged space structure with the l-th eigenfunction serving as the weight. In a previous study, a window size of 20 days was used to focus on quasi-stationary properties (Kim et al., 2008). In this study, we set the window size (substructure) as the minimum sub-seasonal time scale (2 weeks) with a lag of 6 days to analyze the evolution of precipitation in the finer sub-seasonal mode. The number of windows (n in Equation (2)) was 14, from June 1 to August 31.

3 Results

3.1 Boreal Summer Mean and Extreme Precipitation from 1973 to 2022

To determine the interannual variability (IAV) of the JJA mean daily precipitation, we calculated the IAV for each station between 1973 and 2022. Figure 1b depicts the IAV of each ASOS station, the total station mean as well as area-averaged, and the closest grid point values of ERA5. The IAV of the JJA mean precipitation shows large differences among stations. Similarly, in Figure 2a (grey shading), the JJA mean precipitation exhibits large spatial variability among the stations. This result supported the notion that precipitation in South Korea displayed strong spatial variability (Jung et al., 2011). In addition, the station mean of JJA mean precipitation exhibited a slightly increasing trend of 0.65 mm/day over 50-year period, but it was not statistically significant. Spatially, 80% of the total stations (48 of 60 stations) presented an increasing trend in JJA mean precipitation, whereas 20% displayed a decreasing trend, which was not significant (Figure 2b). Specifically, 20% of total stations (12 of 60 stations) showed a greater increasing trend (above 1.5mm/day) over the 50-year period, and most of these stations were concentrated in the northern part of the central region near 38°N and certain coastal regions such as Geoje and Busan.

Five indices were calculated as indicators of extreme precipitation: RX1H, R95p, R99p, R95pF, and R99pF. These indices showed an increasing trend for the 50-year period, but only two had significant increasing trends at a 90% significance level. Figure 2a displays the IAV and trends for the extreme indices from 1973 to 2022. While JJA mean precipitation showed a very slight increase (0.65 mm/day/50 yrs), RX1H presented a very clear increasing trend (7 mm/hr/50 yrs) at a 99% significance level. The linear trends of R95p (R99p) and R95pF (R99pF) were 60.5 mm/50 yrs (37 mm/50 yrs) and 0.5 days/50 yrs (0.2 days/50 yrs) for the same period, respectively. Figures 2c –2g show the spatial distribution of the linear trend for each extreme precipitation index. For RX1H, 50 (10) stations, which accounted for 83.3% (16.7%) of the total stations, showed an increasing (decreasing) trend over the past five decades. Twelve stations (20%) had a significant increasing trend for RX1H (Figure 2c). Most of the significant stations were concentrated in the northern portion of the central region, along the southern coast of Korea. Some stations, such as Imsil and Gumi, were located in inland regions. For R95p, 47 (13) stations, which equate to 78.3% (21.7%), showed increasing (decreasing) trends, and seven stations (approximately 13%) showed significant increasing trends (Figure 2d). In addition to RX1H, the majority of the significant regions were located in the northern portion of the central region. The frequency of R95p occurred more (less) frequently at 43 (17) stations, comprising 71.7% (28.3%) of total stations. Specifically, six stations (10%) displayed increasing trends in R95pF, and their locations were identical to those of R95p, except for one less station (Figure 2e). An increasing (decreasing) trend for R99p was observed at 46 (14) stations, comprising 76.7% (23.3%) of total stations. Specifically, only 3 (5%) stations, namely Incheon, Inje, and Ulleungdo Island, exhibited a significant increasing trend (Figure 2f). Likewise, the frequency of R99p tended to increase (decrease) at 45 (15) stations, with 75% (25%) and six stations (10%) experiencing significant increases. These stations are primarily located in the northern and several coastal regions (Figure 2g). In general, extreme precipitation intensified in the northern portion of the South and certain coastal regions. The exception was the inland basin of Gumi, which also experienced significant increases in RX1H, R95p, and R95pF.

The changes in JJA mean rainfall and each extreme precipitation index between the P1 and P2 revealed the evolution of daily precipitation in South Korea over the past two decades (Figure S1). The increase in the JJA mean precipitation rate was 6.71%. Given that the JJA mean precipitation was 7.63 mm/day for 50-years period, higher summer precipitation was indicated in P2 with a value of 7.72 mm/day, whereas 7.24 mm/day was depicted in P1. The RX1H increased by 12.28%. In addition, R95p (R95pF) tended to increase by approximately 22.85% (20.91%). A notable increase in R99p (R99pF) was observed, at a rate of 43.23% (47.3%), during P2. In addition, South Korea exhibited salient intraseasonal variability; therefore, there was a need to divide the summer season into monthly segments (Ha & Oh, 2019; Jia et al., 2022; Ren et al., 2022). The monthly average precipitation was the highest in July (8.99 mm/day), followed by August (8.55 mm/day), and June (5.26 mm/day). In P1 and P2, JJA mean precipitation increased in July (P1: 8.63 mm/day, P2: 9.92 mm/day) and August (P1: 7.58 mm/day, P2: 8.46 mm/day), whereas it decreased in June (P1: 5.44 mm/day, P2: 4.68 mm/day). R95p (R95pF) and R99p (R99pF) comprised the largest portions at 40.93% (41.12%) and 42.76% (43.16%) in July, respectively, which was followed by August at 38.04% (34.74%) and 39.15% (35.71%), as well as June at 21.03% (24.14%) and 18.09% (21.13%), respectively, for 1973–2022. The amount and frequency of extreme precipitation were mostly concentrated in July. Comparing P1 and P2, this trend became more pronounced in P2. For P1, R95p (R95pF) was 25.17% (27.52%), 38.21% (38.87%), and 36.62% (33.62%) in June, July, and August, respectively. Similarly, R99p (R99pF) constituted 24.37% (27.52%), 39.31% (39.37%), and 36.32% (33.11%) in June, July, and August, respectively. During P2, R95p (R95pF) accounted for 17.05% (19.81%), 49.78% (49.00%), and 33.17% (31.19%) in June, July, and August, respectively. In the case of R99p (R99pF), 15.27% (18.13%), 54.41% (53.51%), and 30.32% (28.36%) were observed in June, July, and August, respectively. In P2, extreme precipitation decreased in June, with the exception of R99pF. Although these four indices increased in July and August, a much further increase was observed in July. Thus, the ratio of extreme indices appeared to decline in August in P2, whereas there was an increase in extreme rainfall occurs in July.

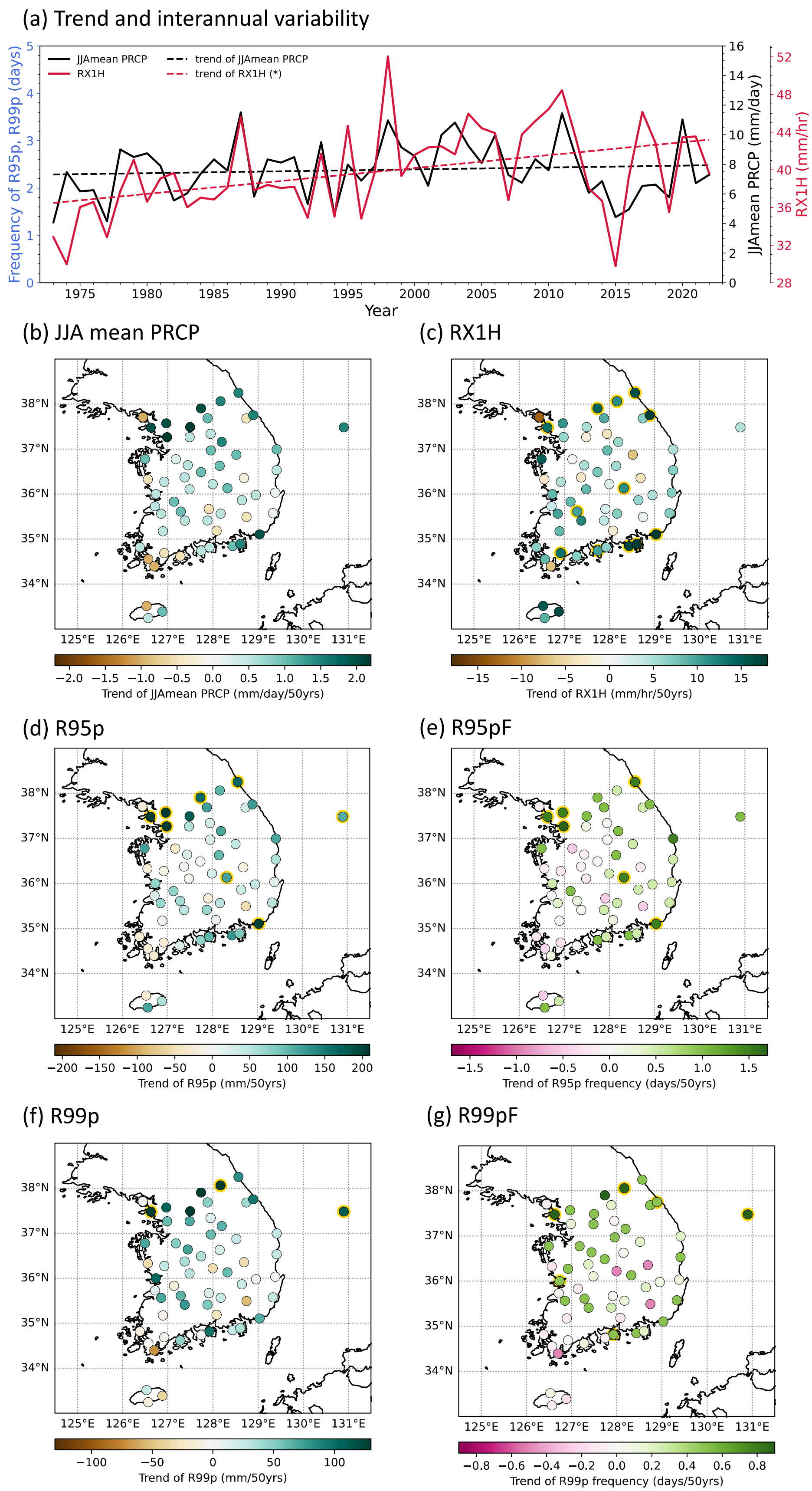

(a) Trend and interannual variability
JJAmean PRCP
RX1H
trend of JJAmean PRCP
trend of RX1H (*)
Frequency of R95p, R99p (days)
JJAmean PRCP (mm/day)
RX1H (mm/hr)
Year
(b) JJA mean PRCP
Trend of JJAmean PRCP (mm/day/50yrs)
(c) RX1H
Trend of RX1H (mm/hr/50yrs)
(d) R95p
Trend of R95p (mm/50yrs)
(e) R95pF
Trend of R95p frequency (days/50yrs)
(f) R99p
Trend of R99p (mm/50yrs)
(g) R99pF
Trend of R99p frequency (days/50yrs)

Figure 2. (a) Time series of boreal summer daily mean precipitation (JJA mean precipitation, solid black line) with its trend (dashed black line) and spatial variability (grey shading) from 1973 to 2022. Extreme indices, hourly-maximum precipitation (RX1H, solid red line) and its trend (dashed red line), as well as the frequencies of R95p (R95pF, light sky-blue bar) and R99p (R99pF, blue bar). The spatial patterns of the trends over the past 50 years are presented in (b) JJA mean precipitation (mm/day/ 50yrs), (c) RX1H (mm/hr/50 yrs), (d) R95p (mm/50 yrs), (e) R95pF (days/50 yrs), (f) R99p (mm/50 yrs), (g) R99pF (days/50 yrs). The enclosed yellow indicates statistical significance at a 90% confidence level.

3.2 Long-term Variations in Mean Temperature and Extreme Precipitation Indices

The EEMD decomposed the mean temperature and extreme precipitation indices into four interannual to interdecadal components (C1 to C4) and one residual trend (Table S3). For 1973–2022, C1 and C2 showed approximately 2.8-year and 5.6-year periodic oscillations, accounting for approximately 55.9% and 20.7% of the total variance, respectively. C3 and C4 show approximately 11.2-year and 28.7-year oscillations and contribute about 10.0% and 4.2% of the total variance, respectively. The residual trend was 9.1%.

To shed light on the long-term changes in the mean temperature and extreme precipitation indices, we defined long-term variations as the sum of decomposed components with more than 10 years of mean periods (C3 and C4) and residuals. Higher temperatures were recorded in high-population regions than in low-population regions (Figure 3a). This result corresponds to the fact that big cities have experienced greater warming because of rapid urbanization and population growth since 1973 (Korea Meteorological Administration, 2020). One salient feature was that long-term changes in mean temperature and PRCPTOT did not occur simultaneously. The mean temperature increased, with multi-decadal fluctuations entering a phase higher than the mean temperature (23.7 °C) from the mid-2000s and stabilizing at 24.4 to 24.5 °C after 2010 (Figure 3a). However, PRCPTOT was in a phase higher than the mean PRCPTOT (698.7 mm) from the mid-1990s to 2010. It peaked at 837 mm in 2002 and decreased to 613.7 mm in 2017. Since then, it has soared (Figure 3b). RX1H, R95p, and R20mm also displayed similar features to PRCPTOT (Figures 3c-e), and the dry day was negatively correlated with PRCPTOT (Figure 3f), indicating that the frequency and intensity of extreme precipitation contributed significantly to PRCPTOT and implying that the increase in the number of dry days and the increase in the frequency and intensity of extreme precipitation during the recent years have greatly influenced the total precipitation in summer. Notably, the long-term changes in PRCPTOT, RX1H, and R95p appeared to be greater in urbanized areas. This result was consistent with that of Wang et al., (2021).

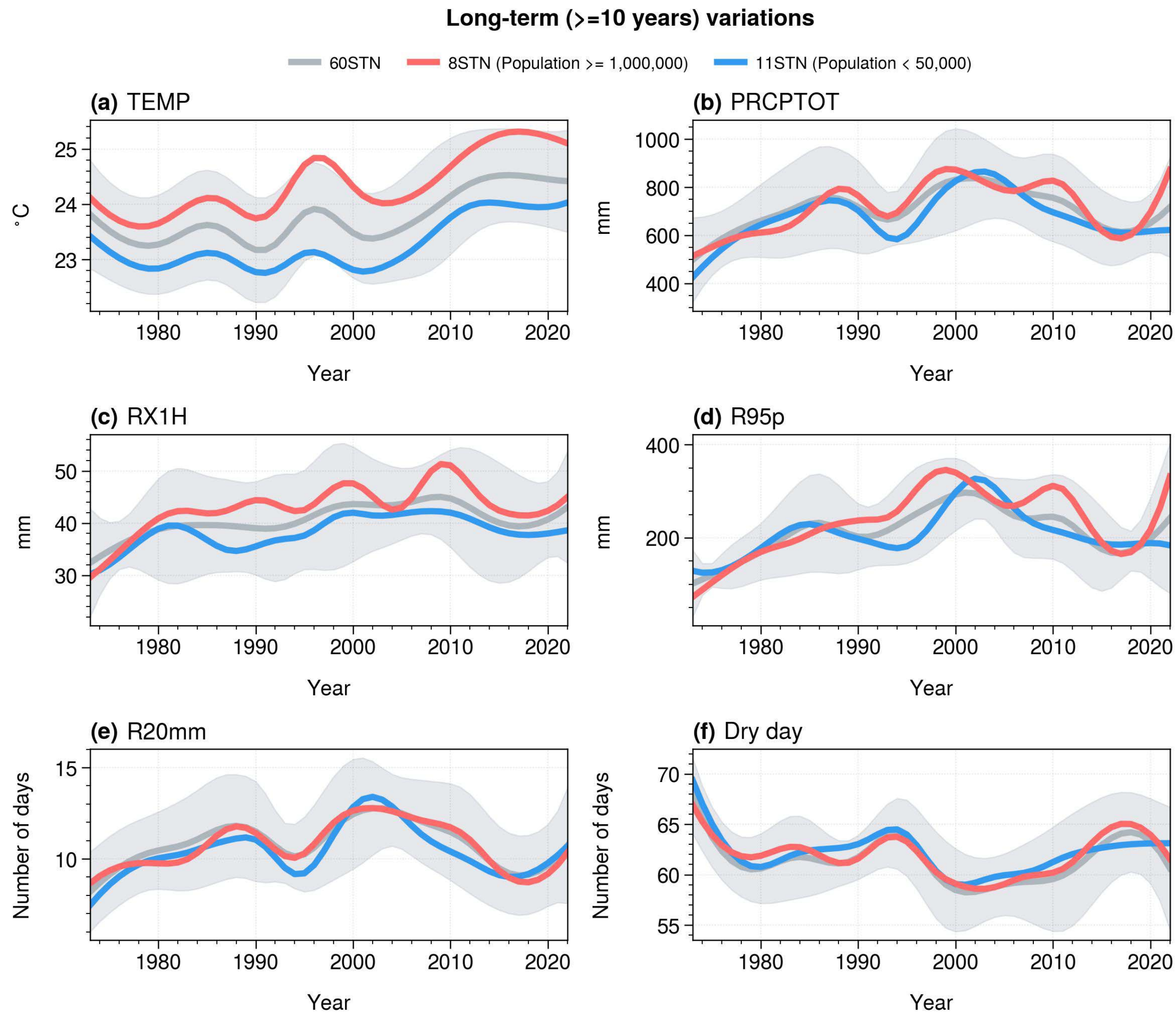

Figure 3. Long-term variations of (a) mean temperature (°C), (b) PRCPTOT (mm), (c) RX1H (mm), (d) R95p (mm), (e) R20mm (days), and (f) dry day (days) from 1973 to 2022 at 60 stations (grey line); 8 stations had a population of 1 million or more (red line), and 11 stations with a population of 50000 or less (blue line). Grey-shaded areas represent one standard error of the mean values from 60 stations. Long-term variations were defined as the sum of decomposed components with mean periods and residuals exceeding 10 years. 8STN (population ≥1,000,000): Seoul, Busan, Incheon, Daegu, Daejeon, Gwangju, Suwon, and Ulsan. 11STN (population < 50,000): Uljin, Wando, Hapcheon, Namhae, Jangheung, Yeongdeok, Sancheong, Boeun, Inje, Imsil, Ulleungdo.

3.3 Sub-seasonal Modes of Precipitation across East Asia during the Boreal Summer

Sub-seasonal evolution is important because the Changma rainband shifts with the summer monsoon. Especially in recent years, ERA5 data could not exactly describe the IAV; therefore, we attempted to compare interdecadal changes between P1 and P2. We utilized the EEOF method on ERA5 daily precipitation over East Asia [120°E–135°E, 25°N–40°N] from

June 1 to August 31 during P1 and P2, respectively, in order to analyze the sub-seasonal mode because the characteristics of the rainfall concentrated in summer were variable even within the season (Figure 4). The first mode of EEOF accounted for 84.9% of the total variance and clearly demonstrated the spatio-temporal evolution of daily precipitation throughout East Asia.

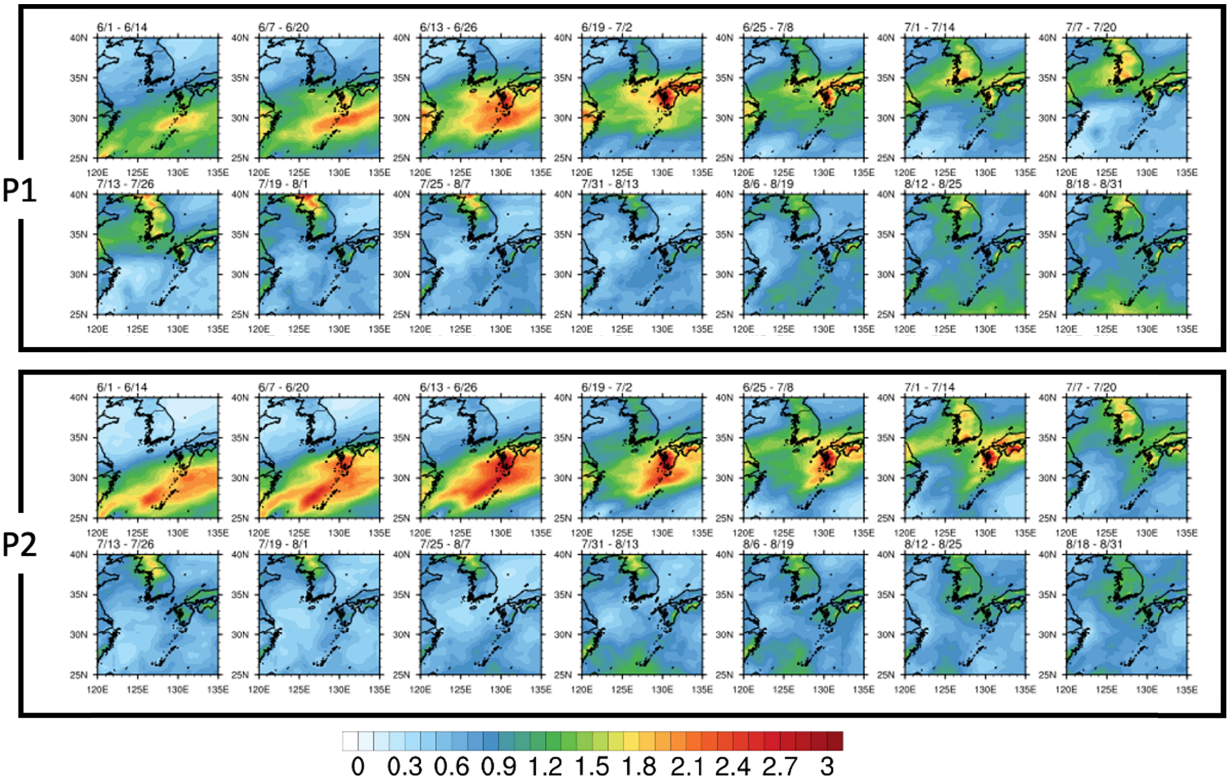

Figure 4. The temporal evolution of the spatial distribution of the first EEOF mode of daily precipitation from June to August for P1 (1973–1992) and P2 (2003–2022).

The stationary precipitation core in the Satsunan Islands, which appeared in the first window (6/1–6/14) near 30°N, developed over time and moved to the KP in the eighth window (7/13–7/26). The spatial distribution of precipitation revealed a core in the north KP and a weak signal in the south KP from the ninth window (mid-July) to the 11th window (early August). In addition to the precipitation that developed locally in the KP, precipitation signals arose south of 30°N in the 12th window. These characteristics appeared in both periods, but the magnitude and disappearance of the precipitation signals were different between P1 and P2.

Compared to the first EEOF mode in P1, a broader and stronger precipitation core appeared in the Satsunan Islands and Okinawa, and a weaker precipitation signal appeared in the KP in the first window in P2. Subsequently, the spatio-temporal evolution shifted northward in the fifth window and rapidly disappeared in the eighth window. The precipitation signal that developed south of 30°N shifted to the earlier two windows compared to that of P1. In the 13th and 14th windows, the local precipitation signal located at the KP became weaker compared to that of P1.

This transition from P1 to P2 demonstrated that throughout the recent two decades, the precipitation core that developed in the early boreal summer (the first window to the fifth window) became stronger with time, whereas the precipitation core generally weakened in the middle period (after the sixth window). Thus, the climatological sub-seasonal mode of precipitation associated with heavy rainfall in the EA region has recently become stronger and shorter.

4 Summary and Discussion

This study analyzed the trend and variability of the summer mean and extreme precipitation from 1973 to 2022. Until the mid-1990s, the ERA5 was similar to the observations. However, since the late 1990s, precipitation from the reanalysis dataset has had a tendency to be underestimated, particularly at the peak of precipitation. This implied that torrential rainfall became more localized, and it was difficult to capture extreme events on a sub-grid scale solely using the reanalysis dataset. Therefore, observational data were invaluable for studying extreme rainfall events. Generally, precipitation indices, in terms of intensity and frequency, showed an increasing trend from 1973 to 2022. One noteworthy result was a significant increase in the hourly-maximum precipitation, whereas the mean precipitation presented a slight increase. In terms of frequency, the number of R99p days became significantly more frequent. Regarding spatial distribution, summer precipitation exhibited greater spatial variability across South Korea. In general, it was illustrated that an increasing trend of mean and extreme precipitation occurred in the northern part of the central region. Additionally, RX1H, R95p, and R95pF increased in some coastal and inland areas.

Changes in mean and extreme precipitation were identified in two periods; P1 and P2. All rainfall indices were higher during the latter period than during the former period. Four extreme indices (R95p, R99p, R95pF, and R99pF) were concentrated in July, August, and June. In P2, this trend strengthened, showing reduced intensity in June (except for R99pF) and strengthening in July and August. Owing to the larger increase in July, extreme precipitation appeared to decrease in August. At the sub-seasonal scale, the precipitation core occurred at 30°N from early to mid-June. Over time, it evolved and shifted to the KP. This core weakened from mid-July to early August, but another precipitation signal reappeared near 30°N by mid-August. During P2, this characteristic manifested with a stronger intensity of the major rainband and earlier timing. In terms of long-term variations, we found that changes in the mean temperature and PRCPTOT occurred at different times. The higher phase of the mean temperature, above the mean value, was reached in the mid-2000s and stabilized in 2010. However, PRCPTOT achieved a higher phase between the mid-1990s and 2010. Similarly, additional extreme precipitation indices, such as RX1H, R95p, and R20mm, showed similar characteristics to PRCPTOT. The dry day had a negative correlation with PRCPTOT. In other words, increases in the intensity and frequency of extreme rainfall had a major impact on the total quantity of summer precipitation in recent years. Moreover, PRCPTOT, RX1H, and R95p were elevated in urbanized regions.

Our results provided a foundation for understanding the mean and extreme precipitation in South Korea in terms of trends, spatio-temporal variability, and long-term variation. First, we emphasized the importance of observational data in the study of heavy rainfall. Second, extreme rainfall had increased more than mean precipitation during the last five decades. In particular, hourly-maximum precipitation increased significantly. Third, extreme precipitation played a greater role in summer precipitation, and several extreme precipitation indices appeared higher in urbanized areas. Finally, the intensification of the rainband occurred sooner over the recent two decades. The results of this study suggested that extreme precipitation events would occur more frequently and with greater intensity in the future. In the event of rapid and extreme rainfall, we should be cautious and well-prepared.

Acknowledgments

This work was supported by a 2021-Year Culture Award Grant of Busan City. We acknowledge Haeun Jeon and Woojin Jung for collecting data.

Open Research

ASOS data are downloadable from https://data.kma.go.kr/data/grnd/selectAsosRltmList.do?pgmNo=36. ERA5 hourly data are available at https://cds.climate.copernicus.eu/cdsapp#!/dataset/reanalysis-era5-single-levels?tab=form. ETOPO1 data can be found at https://www.ncei.noaa.gov/products/etopo-global-relief-model.

References

Alexander, L. v., Zhang, X., Peterson, T. C., Caesar, J., Gleason, B., Klein Tank, A. M. G., Haylock, M., Collins, D., Trewin, B., Rahimzadeh, F., Tagipour, A., Rupa Kumar, K., Revadekar, J., Griffiths, G., Vincent, L., Stephenson, D. B., Burn, J., Aguilar, E., Brunet, M., … Vazquez-Aguirre, J. L. (2006). Global observed changes in daily climate extremes of temperature and precipitation. *Journal of Geophysical Research Atmospheres*, *111*(5). https://doi.org/10.1029/2005JD006290

Allan, R. P., & Soden, B. J. (2008). Atmospheric Warming and the Amplification of Precipitation Extremes. *Science*, *321*(5895), 1481–1484. https://doi.org/10.1126/science.1107142

Allen, M. R., & Ingram, W. J. (2002). Constraints on future changes in climate and the hydrologic cycle. *Nature*. www.nature.com/nature

Amante, C., & Eakins, B. W. (2009). *NOAA Technical Memorandum NESDIS NGDC-24 ETOPO1 1 ARC-MINUTE GLOBAL RELIEF MODEL: PROCEDURES, DATA SOURCES AND ANALYSIS.*

Azam, M., Maeng, S. J., Kim, H. S., Lee, S. W., & Lee, J. E. (2018). Spatial and temporal trend analysis of precipitation and drought in South Korea. *Water (Switzerland)*, *10*(6). https://doi.org/10.3390/w10060765

Bae, G., & Yeung, J. (2022, August 10). *Record rainfall kills at least 9 in Seoul as water floods buildings, submerges cars*. CNN.

Baek, H. J., Kim, M. K., & Kwon, W. T. (2017). Observed short- and long-term changes in summer precipitation over South Korea and their links to large-scale circulation anomalies. *International Journal of Climatology*, *37*(2), 972–986. https://doi.org/10.1002/joc.4753

Borodina, A., Fischer, E. M., & Knutti, R. (2017). Models are likely to underestimate increase in heavy rainfall in the extratropical regions with high rainfall intensity. *Geophysical Research Letters*, *44*(14), 7401–7409. https://doi.org/10.1002/2017GL074530

Chen, J.-M., & Harr, P. A. (1993). Interpretation of Extended Empirical Orthogonal Function (EEOF) Analysis. *Monthly Weather Review*, *121*, 2631–2636.

Chou, C., Chen, C. A., Tan, P. H., & Chen, K. T. (2012). Mechanisms for global warming impacts on precipitation frequency and intensity. *Journal of Climate*, *25*(9), 3291–3306. https://doi.org/10.1175/JCLI-D-11-00239.1

Dave, R., Subramanian, S. S., & Bhatia, U. (2021). Extreme precipitation induced concurrent events trigger prolonged disruptions in regional road networks. *Environmental Research Letters*, *16*(10). https://doi.org/10.1088/1748-9326/ac2d67

Ha, K. J., Moon, S., Timmermann, A., & Kim, D. (2020). Future Changes of Summer Monsoon Characteristics and Evaporative Demand Over Asia in CMIP6 Simulations. *Geophysical Research Letters*, *47*(8). https://doi.org/10.1029/2020GL087492

Ha, K. J., Yeo, J. H., Seo, Y. W., Chung, E. S., Moon, J. Y., Feng, X., Lee, Y. W., & Ho, C. H. (2020). What caused the extraordinarily hot 2018 summer in Korea? *Journal of the Meteorological Society of Japan*, *98*(1), 153–167. https://doi.org/10.2151/jmsj.2020-009

Ha, K.-J., & Oh, H. (2019). Multifaceted Intraseasonal Modes in the East Asian-Western North Pacific Summer Monsoon Climate. In *The Multiscale Global Monsoon System: Vol. Volume 11* (pp. 37–47). WORLD SCIENTIFIC. https://doi.org/doi:10.1142/9789811216602_0004

Ha, K.-J., Yun, K.-S., Jhun, J.-G., & Li, J. (2009). Circulation changes associated with the interdecadal shift of Korean August rainfall around late 1960s. *Journal of Geophysical Research: Atmospheres*, *114*(D4). https://doi.org/https://doi.org/10.1029/2008JD011287

Held, I. M., & Soden, B. J. (2006). Robust Responses of the Hydrological Cycle to Global Warming. *Journal of Climate*, *19*(21), 5686–5699.

Hersbach, H., Bell, B., Berrisford, P., Hirahara, S., Horányi, A., Muñoz-Sabater, J., Nicolas, J., Peubey, C., Radu, R., Schepers, D., Simmons, A., Soci, C., Abdalla, S., Abellan, X., Balsamo, G., Bechtold, P., Biavati, G., Bidlot, J., Bonavita, M., … Thépaut, J. N. (2020). The ERA5 global reanalysis. *Quarterly Journal of the Royal Meteorological Society*, *146*(730), 1999–2049. https://doi.org/10.1002/qj.3803

Ho, C. H., Lee, J. Y., Ahn, M. H., & Lee, H. S. (2003). A sudden change in summer rainfall characteristics in Korea during the late 1970s. *International Journal of Climatology*, *23*(1), 117–128. https://doi.org/10.1002/joc.864

H.-O. Pörtner, D.C. Roberts, M. Tignor, E.S. Poloczanska, K. Mintenbeck, A. Alegría, M. Craig, S. Langsdorf, S. Löschke, v. Möller, A. Okem, & B. Rama. (2022). *IPCC, 2022: Climate Change 2022: Impacts, Adaptation, and Vulnerability. Contribution of Working Group II to the Sixth Assessment Report of the Intergovernmental Panel on Climate Change*.

Hu, W., Chen, L., Shen, J., Yao, J., He, Q., & Chen, J. (2022). Changes in Extreme Precipitation on the Tibetan Plateau and Its Surroundings: Trends, Patterns, and Relationship with Ocean Oscillation Factors. *Water*, *14*(16). https://doi.org/10.3390/w14162509

Jeong, Y., Nam, S., Kwon, J.-I., Uppara, U., & Jo, Y.-H. (2022). Surface Warming Slowdown With Continued Subsurface Warming in the East Sea (Japan Sea) Over Recent Decades (2000–2014). *Frontiers in Marine Science*, *9*. https://doi.org/10.3389/fmars.2022.825368

Jia, Z., Zheng, Z., Feng, G., & Tong, M. (2022). The Intraseasonal Variations of the Leading Mode of Summer Precipitation Anomalies in Meiyu Area of East Asia. *Atmosphere*, *13*(2). https://doi.org/10.3390/atmos13020217

Jung, H. S., Choi, Y., Oh, J. H., & Lim, G. H. (2002). Recent trends in temperature and precipitation over South Korea. *International Journal of Climatology*, *22*(11), 1327–1337. https://doi.org/10.1002/joc.797

Jung, I. W., Bae, D. H., & Kim, G. (2011). Recent trends of mean and extreme precipitation in Korea. *International Journal of Climatology*, *31*(3), 359–370. https://doi.org/10.1002/joc.2068

Kharin, V. v., Zwiers, F. W., Zhang, X., & Hegerl, G. C. (2007). Changes in temperature and precipitation extremes in the IPCC ensemble of global coupled model simulations. *Journal of Climate*, *20*(8), 1419–1444. https://doi.org/10.1175/JCLI4066.1

Kim, H., Lee, J.-H., Park, H.-J., & Heo, J.-H. (2021). Assessment of temporal probability for rainfall-induced landslides based on nonstationary extreme value analysis. *Engineering Geology*, *294*. https://doi.org/https://doi.org/10.1016/j.enggeo.2021.106372

Kim, J., Choi, J., Choi, C., & Park, S. (2013). Impacts of changes in climate and land use/land cover under IPCC RCP scenarios on streamflow in the Hoeya River Basin, Korea. *Science of the Total Environment*, *452–453*, 181–195. https://doi.org/10.1016/j.scitotenv.2013.02.005

Kim, J. H., Wu, C. C., Sui, C. H., & Ho, C. H. (2012). Tropical cyclone contribution to interdecadal change in summer rainfall over South China in the early 1990s. *Terrestrial, Atmospheric and Oceanic Sciences*, *23*(1), 49–58. https://doi.org/10.3319/TAO.2011.08.26.01(A)

Kim, K. Y., Kitoh, A., & Ha, K. J. (2008). The SST-forced predictability of the sub-seasonal mode over East Asia with an atmospheric general circulation model. *International Journal of Climatology*, *28*(12), 1599–1606. https://doi.org/10.1002/joc.1655

Kim, S., & Ha, K.-J. (2021). Interannual and decadal covariabilities in East Asian and Western North Pacific summer rainfall for 1979–2016. *Climate Dynamics*, *56*(3), 1017–1033. https://doi.org/10.1007/s00382-020-05517-7

Korea Meteorological Administration. (2020). *Korean Climage Change Assessment Report 2020-The Physical Science Basis-Summary for Policymakers*.

Lee, J.-Y., Kwon, M., Yun, K.-S., Min, S.-K., Park, I.-H., Ham, Y.-G., Jin, E. K., Kim, J.-H., Seo, K.-H., Kim, W., Yim, S.-Y., & Yoon, J.-H. (2017). The long-term variability of Changma in the East Asian summer monsoon system: A review and revisit. *Asia-Pacific Journal of Atmospheric Sciences*, *53*(2), 257–272. https://doi.org/10.1007/s13143-017-0032-5

Lee, M. H., Ho, C. H., Kim, J., & Song, C. K. (2012). Assessment of the changes in extreme vulnerability over East Asia due to global warming. *Climatic Change*, *113*(2), 301–321. https://doi.org/10.1007/s10584-011-0345-9

Meyer, J., Neuper, M., Mathias, L., Zehe, E., & Pfister, L. (2021). More frequent flash flood events and extreme precipitation favouring atmospheric conditions in temperate regions of Europe. *Hydrology and Earth System Sciences*. https://doi.org/10.5194/hess-2021-628

Min, S. K., Son, S. W., Seo, K. H., Kug, J. S., An, S. il, Choi, Y. S., Jeong, J. H., Kim, B. M., Kim, J. W., Kim, Y. H., Lee, J. Y., & Lee, M. I. (2015). Changes in weather and climate extremes over Korea and possible causes: A review. In *Asia-Pacific Journal of Atmospheric Sciences* (Vol. 51, Issue 2, pp. 103–121). Korean Meteorological Society. https://doi.org/10.1007/s13143-015-0066-5

Min, S. K., Zhang, X., Zwiers, F. W., & Hegerl, G. C. (2011). Human contribution to more-intense precipitation extremes. *Nature*, *470*(7334), 378–381. https://doi.org/10.1038/nature09763

Moberg, A., Jones, P. D., Lister, D., Walther, A., Brunet, M., Jacobeit, J., Alexander, L. v, Della-Marta, P. M., Luterbacher, J., Yiou, P., Chen, D., Tank, A. M. G. K., Saladié, O., Sigró, J., Aguilar, E., Alexandersson, H., Almarza, C., Auer, I., Barriendos, M., … Xoplaki, E. (2006). Indices for daily temperature and precipitation extremes in Europe analyzed for the period 1901–2000. *Journal of Geophysical Research: Atmospheres*, *111*(D22). https://doi.org/https://doi.org/10.1029/2006JD007103

Moon, M., & Ha, K. J. (2021). Abnormal Activities of Tropical Cyclones in 2019 Over the Korean Peninsula. *Geophysical Research Letters*, *48*(7). https://doi.org/10.1029/2020GL090784

Ning, G., Luo, M., Zhang, Q., Wang, S., Liu, Z., Yang, Y., Wu, S., & Zeng, Z. (2021). Understanding the Mechanisms of Summer Extreme Precipitation Events in Xinjiang of Arid Northwest China. *Journal of Geophysical Research: Atmospheres*, *126*(15). https://doi.org/10.1029/2020JD034111

O'Gorman, P. A., & Schneider, T. (2009). The physical basis for increases in precipitation extremes in simulations of 21st-century climate change. *Proceedings of the National Academy of Sciences of the United States of America*, *106*(35), 14773–14777. https://doi.org/10.1073/pnas.0907610106

Park, B. J., Kim, Y. H., Min, S. K., Kim, M. K., Choi, Y., Boo, K. O., & Shim, S. (2017). Long-Term Warming Trends in Korea and Contribution of Urbanization: An Updated Assessment. *Journal of Geophysical Research: Atmospheres*, *122*(20), 10,637-10,654. https://doi.org/10.1002/2017JD027167

Park, C., Son, S.-W., Kim, H., Ham, Y.-G., Kim, J., Cha, D.-H., Chang, E.-C., Lee, G., Kug, J.-S., Lee, W.-S., Lee, Y.-Y., Lee, H. C., & Lim, B. (2021). Record-Breaking Summer Rainfall in South Korea in 2020: Synoptic Characteristics and the Role of Large-Scale Circulations. *Monthly Weather Review*, *149*, 3085–3100. https://doi.org/10.1175/MWR-D

Park, H. L., Seo, K. H., & Son, J. H. (2015). Development of a dynamics-based statistical prediction model for the Changma onset. *Journal of Climate*, *28*(17), 6647–6666. https://doi.org/10.1175/JCLI-D-14-00502.1

Pei, L., Xia, J., Yan, Z., & Yang, H. (2017). Assessment of the Pacific decadal oscillation's contribution to the occurrence of local torrential rainfall in north China. *Climatic Change*, *144*(3), 391–403. https://doi.org/10.1007/s10584-016-1610-8

Ren, Q., Liu, F., Wang, B., Yang, S., Wang, H., & Dong, W. (2022). Origins of the Intraseasonal Variability of East Asian Summer Precipitation. *Geophysical Research Letters*, *49*(4). https://doi.org/10.1029/2021GL096574

Ryan, C., Curley, M., Walsh, S., & Murphy, C. (2022). Long-term trends in extreme precipitation indices in Ireland. *International Journal of Climatology*, *42*(7), 4040–4061. https://doi.org/https://doi.org/10.1002/joc.7475

Seo, K.-H., Son, J.-H., & Lee, J.-Y. (2011). A New Look at Changma. *Atmosphere*, *21*, 109–121.

Seo, Y. W., Ha, K. J., & Park, T. W. (2021). Feedback attribution to dry heatwaves over East Asia. *Environmental Research Letters*, *16*(6). https://doi.org/10.1088/1748-9326/abf18f

Soon-il, A., Kyung-Ja, H., Kyong-Hwan, S., Sang-Wook, Y., Seung-Ki, M., & Chang-Hoi, H. (2011). A Review of Recent Climate Trends and Causes over the Korean Peninsula. *Journal of Climate Change Research(한국기후변화학회지)*, *2*(4), 237–251. www.dbpia.co.kr

Trenberth, K. E., Dai, A., Rasmussen, R. M., & Parsons, D. B. (2003). THE CHANGING CHARACTER OF PRECIPITATION. *Bulletin of the American Meteorological Society*, *84*(9), 1205–1218.

Wang, B., Biasutti, M., Byrne, M. P., Castro, C., Chang, C.-P., Cook, K., Fu, R., Grimm, A. M., Ha, K.-J., Hendon, H., Kitoh, A., Krishnan, R., Lee, J.-Y., Li, J., Liu, J., Moise, A., Pascale, S., Roxy, M. K., Seth, A., … Zhou, T. (2021). Monsoons Climate Change Assessment. *Bulletin of the American Meteorological Society*, *102*(1), E1–E19. https://doi.org/10.1175/BAMS-D-19-0335.1

Wu, Z., & Huang, N. E. (2004). A study of the characteristics of white noise using the empirical mode decomposition method. *Proceedings of the Royal Society of London. Series A: Mathematical, Physical and Engineering Sciences*, *460*(2046), 1597–1611. https://doi.org/10.1098/rspa.2003.1221

Wu, Z., & Huang, N. E. (2009). Ensemble empirical mode decomposition: a noise-assisted data analysis method. *Advances in Adaptive Data Analysis*, *01*(01), 1–41. https://doi.org/10.1142/S1793536909000047

Yao, C., Yang, S., Qian, W., Lin, Z., & Wen, M. (2008). Regional summer precipitation events in Asia and their changes in the past decades. *Journal of Geophysical Research Atmospheres*, *113*(17). https://doi.org/10.1029/2007JD009603

Yun, J., Ha, K.-J., & Jo, Y.-H. (2018). Interdecadal changes in winter surface air temperature over East Asia and their possible causes. *Climate Dynamics*, *51*(4), 1375–1390. https://doi.org/10.1007/s00382-017-3960-y